SCIENTIFIC REPORTS

OPEN

SUBJECT AREAS:
TISSUE ENGINEERING
REGENERATIVE MEDICINE

Received
29 October 2013

Accepted
12 December 2013

Published
14 January 2014

Correspondence and requests for materials should be addressed to G.V.-N. (gv2131@columbia.edu)

Electrical stimulation enhances cell migration and integrative repair in the meniscus

Xiaoning Yuan[1], Derya E. Arkonac[1], Pen-hsiu Grace Chao[2] & Gordana Vunjak-Novakovic[1]

[1]Department of Biomedical Engineering, Columbia University, New York NY, USA, [2]Institute of Biomedical Engineering, School of Medicine and School of Engineering, National Taiwan University, Taipei, Taiwan.

Electrical signals have been applied towards the repair of articular tissues in the laboratory and clinical settings for over seventy years. We focus on healing of the meniscus, a tissue essential to knee function with limited innate repair potential, which has been largely unexplored in the context of electrical stimulation. Here we demonstrate for the first time that electrical stimulation enhances meniscus cell migration and integrative tissue repair. We optimize pulsatile direct current electrical stimulation parameters on cells at the micro-scale, and apply these to healing of full-thickness defects in explants at the macro-scale. We report increased expression of the adenosine A_{2b} receptor in meniscus cells after stimulation at the micro- and macro-scale, and propose a role for $A_{2b}R$ in meniscus electrotransduction. Taken together, these findings advance our understanding of the effects of electrical signals and their mechanisms of action, and contribute to developing electrotherapeutic strategies for meniscus repair.

Electric fields are known to guide the development and regeneration of many tissues, including cartilage[1–3]. However, the exact roles of electrical signals in regulating the biosynthetic activity and homeostasis of articular tissues remain elusive, although preclinical and clinical studies have demonstrated superior healing following their application[4–6]. The meniscus is of particular interest, as knee arthroscopy for meniscus intervention is the most performed procedure by orthopaedic surgeons[7]. In the past, the entire meniscus was routinely removed by total meniscectomy, but long-term outcomes have since demonstrated that the incidence and severity of osteoarthritis is proportional to the amount of tissue removed[8]. Moreover, the extent of intrinsic repair after surgery is largely determined by the location of the injury: while meniscus tears in the vascularized, outer tissue region can undergo repair, those in the avascular inner region, similar to cartilage, do not heal, and the damaged tissue must instead be removed[9]. Therefore, general wisdom in orthopaedics has been that vascularity is necessary for healing, and the regional variation that exists within the meniscus has led to novel approaches to overcome the limited treatment options for injuries in the inner region.

The biochemical composition of the meniscus also varies by region, with predominantly type I collagen in the more fibrous outer region, and a mixture of types I and II collagen in the more cartilaginous inner region[10]. The bulk of the remaining extracellular matrix (ECM) is composed of negatively charged glycosaminoglycans (GAGs)[11], which hydrate the tissue, contribute to its compressive properties, and also allow for electrical activity[12]. After meniscus injury, increases in GAG levels in the synovial fluid peak early, and persist out to four years after injury[13]. The synovial environment after injury also has elevated levels of IL-1 and TNF-α[14–16], which act in concert to increase the production of nitric oxide (NO), prostaglandin E_2 (PGE_2), and matrix metalloproteinases (MMPs), increase the release of GAGs, and decrease the synthesis of collagen in the meniscus[17–19]. The full-thickness defect model in explants has been employed extensively in the study of meniscus repair in the presence of IL-1 and TNF-α, demonstrating dose-dependent decreases in integration strength and tissue repair over sustained supplementation[20], and long-term potentiation of effects even after acute exposure[21]. The application of dynamic loading on meniscus explants in the presence of IL-1 was found in turn to combat the cytokine's inflammatory effects on integrative repair[22].

The endogenous electrical potentials during physiological loading of articular cartilage have been studied using theoretical[23–25] and experimental[26–28] models, and these native electrical signals have been implicated in transducing mechanical signals to cells within tissues[26,29,30]. A variety of electrical stimulation modalities investigated in 2-D and 3-D models of cartilage *in vitro* and cartilage repair *in vivo*[4–6] were shown to significantly increase cell proliferation[31,32] and GAG synthesis[33,34], upregulate the expression of ECM genes[35], and reduce the production of

inflammatory mediators such as IL-1 and MMPs[36]. However, questions remain as to how electrical signals influence cells and propagate their effects. The adenosine receptors have been implicated in the electrotransduction of pulsed electromagnetic fields in cartilage[37,38]. Stimulation of the high-affinity A_{2a} and low-affinity A_{2b} adenosine receptors resulted in elevated cyclic AMP[39] and subsequent activation of anti-inflammatory pathways via protein kinase A and EPAC, which in turn lead to the suppression of NO and PGE_2[40] and downstream feedback inhibition of TNF-α and IL-1β[41]. We therefore hypothesized that electrical stimulation will enhance repair of the meniscus and control the inflammatory events underlying tissue degradation.

Given the wealth of background information on electrical stimulation, inflammation, and adenosine receptor signaling in cartilage repair, it may come as a surprise that very little published information exists in the context of the meniscus. Only recently, meniscus cells from the outer region were found to migrate more quickly in 2-D culture than inner cells, in the presence of static direct current (DC) fields[42]. However, electrical stimulation studies have demonstrated a disparity in migration behavior between 2-D and more physiologically relevant 3-D environments[43]. Moreover, pulsatile electric fields (EFs) are already used in the clinical setting for related conditions[44,45]. At this time, the effects of applied EFs on meniscus cells and subsequent development of novel repair strategies are only beginning to be understood. We investigated the effects of pulsatile direct current electric field stimulation on meniscus cell migration in a micropatterned 3-D hydrogel system. Our micro-scale system also enabled study of the paracrine signaling between meniscus and vascular endothelial cells, in concert with electrical stimulation. Electric fields are known to induce VEGF receptor signaling in endothelial cells[46], so we expected that patterns of meniscus cell migration that result from the differences in intrinsic vascularity within the tissue will be further enhanced by interactions between electric fields and endothelial cells. Moreover, little is known about the signal transduction pathways that respond to electrical stimuli in meniscus cells. Screening and optimization of stimulation parameters at the micro-scale enabled us to identify potential pathways involved in electrotransduction. By translating from the micro- to the macro-scale, we established stimulation regimes that enhanced integrative repair of full-thickness defects in meniscus, and demonstrated promising therapeutic effects of electrical stimulation on meniscus healing.

Results

Electrical stimulation has differential effects on meniscus cell migration. Electrical stimulation of the meniscus was investigated using three distinctly different yet related experimental model systems in which inner and outer meniscus cells or explants were subjected to pulsatile direct current electrical stimulation: (a) micropatterned three-dimensional hydrogels with encapsulated inner or outer meniscus cells, (b) micropatterned 3-D hydrogels with spatially distributed meniscus and endothelial cells, and (c) a macroscopic *in vitro* model of meniscus healing (Fig. 1). When cultured in the micropatterned 3-D hydrogel system, meniscus cells migrated over six days of culture, with the stimulated cells demonstrating enhanced migration relative to non-stimulated control cells (Fig. 2a). Notably, both inner and outer meniscus cells exhibited similar increases in migration with applied electrical signals at 3 V/cm, 1 Hz, 2 ms pulse duration (Fig. 2b), despite the variation in repair response between their respective tissue regions. When injected charge, or the total amount of charge delivered during one stimulus pulse, was maintained at a constant field strength of 3 V/cm, further increases in cell migration were gained as the frequency of stimulation increased to 10 Hz and the pulse duration decreased to 0.2 ms (Fig. 2c). The combinations of 3 V/cm, 0.1 Hz, 20 ms pulse duration, and 3 V/cm, 100 Hz, 0.02 ms pulse duration were also tested, but the longer pulse duration associated with 0.1 Hz led to a more rounded, quiescent cell appearance rather than the spread-out, migrating cell phenotype seen at the channel edge. The increase in frequency to 100 Hz did not markedly improve the migration behavior of inner or outer meniscus cells, likely a result of too brief of a refractory period for cells to fully respond to subsequent stimulation pulses.

No apparent difference in positive BrdU staining, indicative of cellular proliferation, was apparent between the inner and outer cells, with and without stimulation (Fig. 2d), suggesting that differences in cell motility over six days of culture were not the result of proliferation only. Finally, type I collagen, a key ECM component throughout the meniscus, exhibited trends of elevated gene expression in both inner and outer cells when the frequency of electrical stimulation was increased while maintaining constant injected charge (Fig. 2e).

Cooperative action of electrical stimulation and endothelial cells on meniscus cell migration. Co-culture with human umbilical vein endothelial cells (HUVECs) was investigated in the context of regional variation in healing between the inner and outer meniscus. Notably, HUVECs further potentiated the effects of electrical stimulation on meniscus cell migration (Fig. S1). Stimulating HUVECs alone in the hydrogel system led to increased expression of *EDN1, PDGFA,* and *PDGFB* genes (Fig. 3a), which encode key angiogenic factors (endothelin-1, PDGF-A, B) that modulate the behaviors of chondrocytes[47] and meniscus cells[48], suggesting a dual role of electrical stimulation in upregulating angiogenic factors that specifically enhance meniscus cell migration, in addition to promoting cell migration in general. Although meniscus cells alone exhibited greater migration in response to the 3 V/cm, 10 Hz, 0.2 ms pulse duration regime, meniscus cell migration in co-culture with HUVECs at 10 Hz stimulation was not significantly greater than without HUVECs at 10 Hz, but was significantly greater than in non-stimulated meniscus cells with HUVECs (Fig. 3b). The cooperative action of stimulation and co-culture was observed in the 3 V/cm, 1 Hz, 2 ms pulse duration regime (Fig. 3b), suggesting that frequency-dependent interactions between chemical and electrical stimuli require optimization for collaborative effects. In this system, the expression of angiogenic factors by HUVECs was upregulated dramatically with stimulation at 1 Hz as compared to non-stimulated controls, whereas the effect of increasing frequency from 1 to 10 Hz was much smaller (Fig. 3a). These findings may account for the positive trends seen in meniscus cell migration with co-culture at 1 Hz stimulation that were not apparent at 10 Hz.

Using the 1 Hz stimulation regime, gene expression profiles of the meniscus cells were further investigated to elucidate how stimulation and co-culture cooperate to enhance migration. As seen in cultures of meniscus cells with electrical stimulation alone, both inner and outer cells showed increases in *COL1A2* expression in response to combined stimulation at 1 Hz and co-culture with HUVECs (Fig. 3c). Although inner and outer meniscus cells demonstrated similar migration behavior in co-culture with HUVECs, they do so in response to different angiogenic factors secreted by endothelial cells, as seen at the gene expression level. Both types of cells responded to stimulation in co-culture with HUVECs by increased expression of *EDNRA*, encoding endothelin receptor type A (Fig. 3c). However, outer cells responded to the secretion of PDGF isoforms by HUVECs with increased expression of *PDGFRA* and *PDGFRB*, encoding PDGF receptors α and β, while no such changes were detected for inner cells. These results demonstrate that electrical stimulation and endothelial cells collaborate to activate meniscus cell receptors at the gene expression level, suggesting potential synergy between the biophysical and biochemical stimuli.

Electrical stimulation enhanced integrative repair of meniscus explants. Using a macroscopic *in vitro* model of meniscus healing, translation of the micro-scale findings to the macro-scale revealed a significant increase in the integration strength of full-thickness

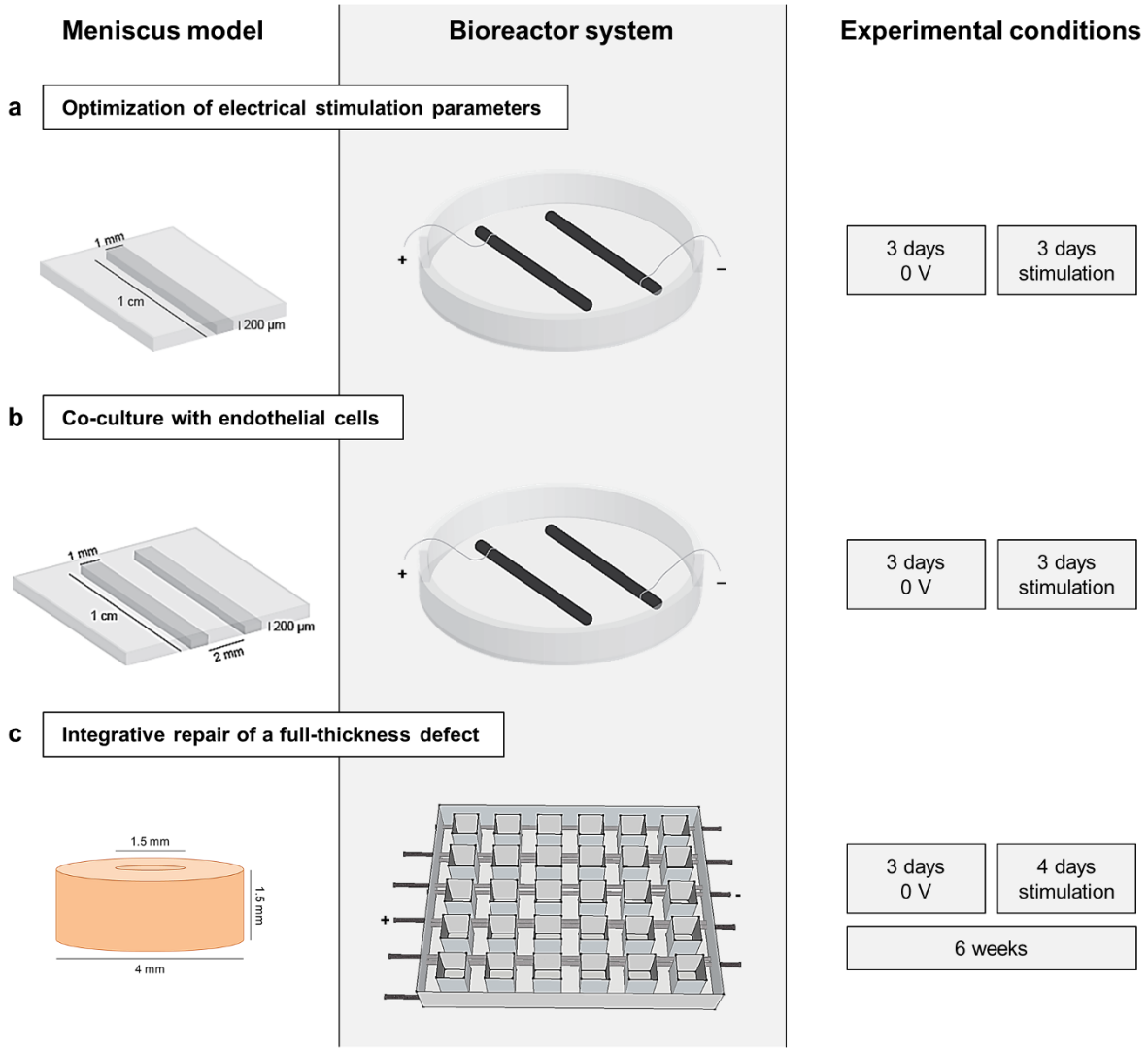

Figure 1 | Electrical stimulation of meniscus. (a) Optimization of electrical stimulation parameters in a micropatterned 3-D hydrogel system for cell migration. Inner or outer meniscus cells were encapsulated on plastic slides in a 1.8% fibrin channel (3.5×10^6 cells/mL) and covered by a second layer of 1.8% fibrin to enable migration. After 3 days of pre-culture, slides were transferred into custom bioreactors with carbon electrodes spaced 2.5 cm apart, for 3 days of stimulation. (b) Co-culture of meniscus cells with endothelial cells. Human umbilical vein endothelial cells (HUVECs) and inner or outer meniscus cells (3.5×10^6 cells/mL) were individually encapsulated on slides in parallel fibrin channels, left and right, respectively, and cultured for 3 days of pre-culture and 3 days of stimulation. (c) Juvenile bovine meniscus explants were punched with central cores of 1.5 mm diameter and immediately replaced to simulate a full-thickness defect. Explants were stimulated four days a week over six weeks of culture in a custom bioreactor system, consisting of a 5×6 array with carbon electrodes spaced 1 cm apart.

defects in explants stimulated at 3 V/cm, 10 Hz, 0.2 ms pulse duration, after six weeks of culture (Fig. 4a). Stimulation at 1 Hz, 2 ms pulse duration initially corresponded to decreases in integration strength over the first four weeks of culture, but surpassed control conditions without stimulation by day 42, albeit to a lesser extent than stimulation at 10 Hz. The underlying basis for the enhanced integration strength of defects in explants stimulated at 10 Hz was further explored by assaying for biochemical content and visualizing the distribution of cells and ECM within the tissue. The overall biochemical content of explants without stimulation decreased throughout six weeks of culture, consistent with previous studies of explant stability in long-term culture, in the absence of growth factor supplementation[49,50] (Fig. 4b). However, the GAG and OHP content of explants stimulated at 10 Hz was not significantly different than at day 0, in comparison to explants without stimulation, which were significantly lower than initial values (Fig. 4b). In general, stimulation led to significant upward trends in DNA and OHP content of explants after six weeks of culture, as compared to explants without stimulation (Fig. 4b).

Histological evaluation revealed that the defect interface appeared more closely apposed in explants stimulated at 10 Hz than in control explants (Fig. 4c). Specifically, newly synthesized matrix was observed at the interface, containing sulfated GAGs and collagens, as evidenced by Alcian blue and Picrosirius red staining, respectively. BrdU labeling was performed to assess the effects of electrical stimulation on cell proliferation, yielding more BrdU-positive cells at the interface of stimulated explants, and indicating a moderate role of electrical stimulation in triggering cell proliferation in explants over long-term culture. Taken together, these data suggest that in addition to tissue repair, electrical stimulation acts to maintain cells and overall ECM composition, and prevent explant degradation *in vitro*.

Anti-inflammatory effects of electrical stimulation on meniscus explants. Evaluation of the components from media collected

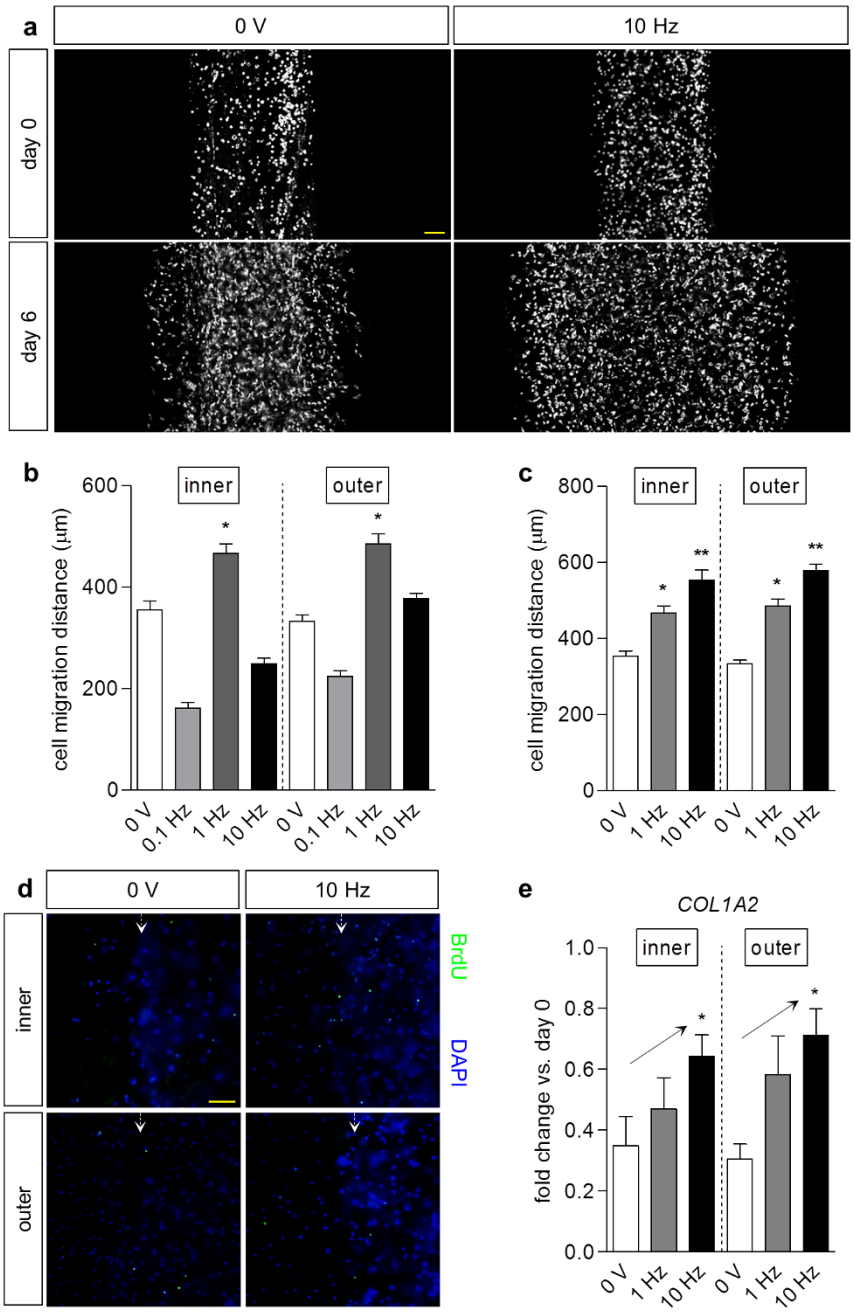

Figure 2 | Electrical stimulation enhanced meniscus cell migration. (a) Representative images of inner meniscus cell migration in a micropatterned hydrogel system with (10 Hz) and without (0 V) electrical stimulation, before (day 0) and after 3 days of pre-culture and 3 days (day 6) of stimulation (3 V/cm, 10 Hz, 0.2 ms pulse duration) or no stimulation (0 V). Scale bar: 200 μm. (b) Optimization of stimulation frequency. Parameters were held constant at 3 V/cm, 2 ms pulse duration, with varying frequency (0.1, 1, 10 Hz). Migration distances at day 6 demonstrated increases for inner and outer meniscus cells at 1 Hz versus cells without stimulation (0 V). * $p < 0.05$ vs. 0 V; $n = 38$–194. (c) Maintenance of charge injection. Field strength was held constant at 3 V/cm, with varying frequency and pulse duration. A higher frequency (10 Hz) and shorter pulse duration (0.2 ms) further enhanced inner and outer meniscus cell migration at day 6. * $p < 0.05$ vs. 0 V; ** $p < 0.05$ vs. 0 V, 1 Hz; $n = 68$–252. (d) Immunofluorescence staining of migrating inner and outer cells at day 6 with (3 V/cm, 10 Hz, 0.2 ms pulse duration) or without (0 V) stimulation, against BrdU for proliferating cells and DAPI for nuclei. No overt differences in cell proliferation were apparent between the cell types with and without stimulation. Scale bar: 200 μm. (e) Fold change ($2^{-\Delta\Delta C_T}$) in gene expression of *COL1A2* in meniscus cells at day 6 relative to cells at day 0, respectively, both normalized to *GAPDH*. Increasing frequency of stimulation with maintenance of injected charge (3 V/cm, 1 Hz, 2 ms or 3 V/cm, 10 Hz, 0.2 ms pulse duration) led to upward trends in gene expression. * $p < 0.05$ for linear trend; $n = 5$–10.

throughout six weeks of culture revealed increases in endogenous TNF-α and IL-1β production by explants without stimulation, compared to those receiving stimulation at 3 V/cm, 10 Hz, 0.2 ms pulse duration, particularly within the first four weeks (Fig. S2a, b). The elevated cytokine levels in explants without stimulation corresponded with changes in NO production (Fig. S2c), MMP activity (Fig. S2d), and GAG release (Fig. S2e), which were typical of catabolic degradation: in comparison to stimulated explants, greater NO production, MMP activity, and GAG release were detected in explants without stimulation, suggestive of an anti-inflammatory, anti-catabolic, and stabilizing effect of electrical stimulation in long-term culture *in*

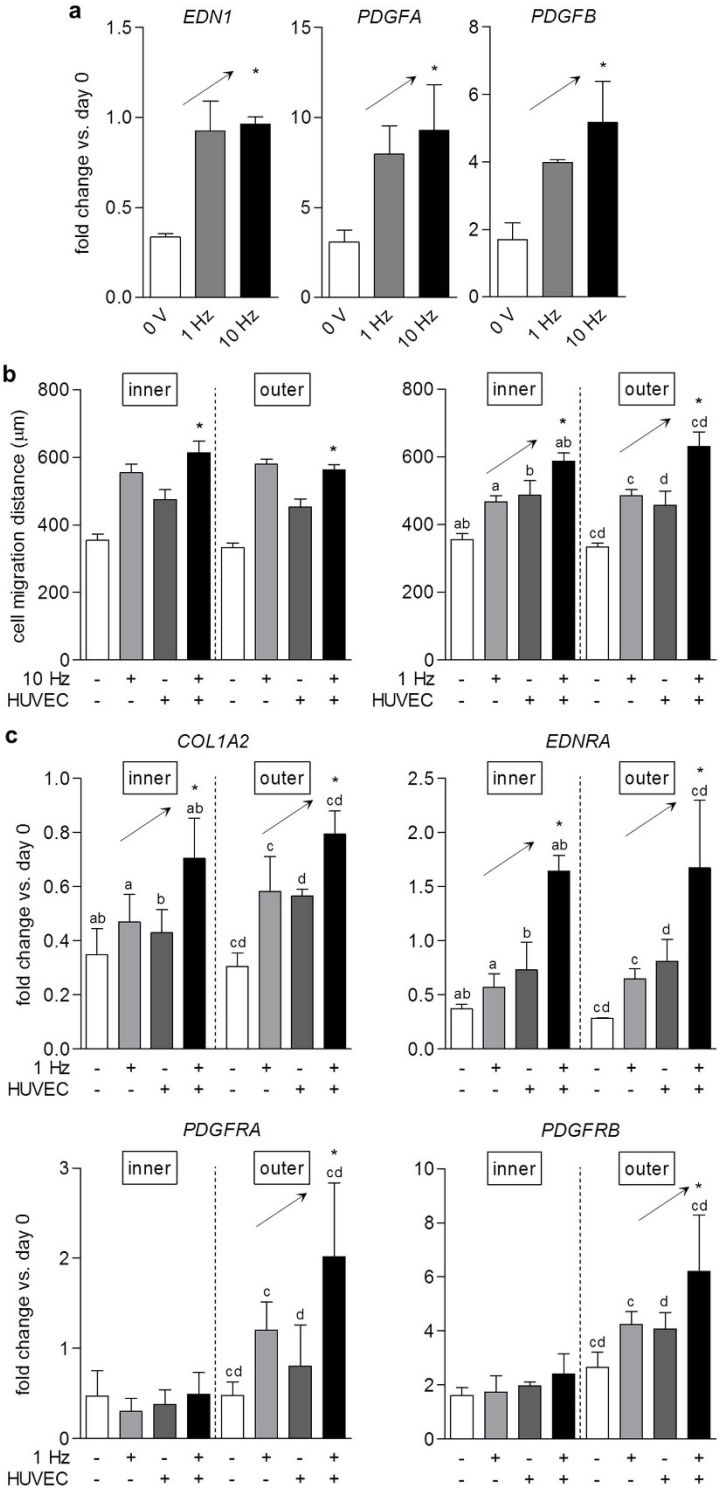

Figure 3 | Cooperative action of electrical stimulation and endothelial cells on meniscus cell migration. (a) Fold change ($2^{-\Delta\Delta C_T}$) in gene expression of *EDN1, PDGFA*, and *PDGFB* in HUVECs at day 6 relative to cells at day 0, respectively, both normalized to *GAPDH*. Increasing frequency of stimulation with maintenance of injected charge (3 V/cm, 1 Hz, 2 ms or 3 V/cm, 10 Hz, 0.2 ms pulse duration) led to upward trends in gene expression. * $p < 0.05$ for linear trend; $n = 3$–4. (b) Optimization of electrical stimulation parameters for co-culture of HUVECs and meniscus cells. Meniscus cell migration with HUVECs and stimulation at 3 V/cm, 10 Hz, 0.2 ms pulse duration (10 Hz) was greater than with HUVECs alone at day 6 (left). * $p < 0.05$ vs. + HUVEC; $n = 37$–154. Meniscus cell migration with HUVECs and stimulation at 3 V/cm, 1 Hz, 2 ms pulse duration (1 Hz) demonstrated cooperative, upward trends with the addition of each stimulus at day 6 (right). * $p < 0.05$ for linear trend (analysis of groups indicated by the same letter); $n = 24$–194. (c) Fold change ($2^{-\Delta\Delta C_T}$) in gene expression of *COL1A2, EDNRA, PDGFRA*, and *PDGFRB* in meniscus cells at day 6 relative to cells at day 0, respectively, both normalized to *GAPDH*. Increasing frequency of stimulation with maintenance of injected charge (3 V/cm, 1 Hz, 2 ms or 3 V/cm, 10 Hz, 0.2 ms pulse duration) led to upward trends in gene expression. * $p < 0.05$ for linear trend (analysis of groups indicated by the same letter); $n = 3$–10.

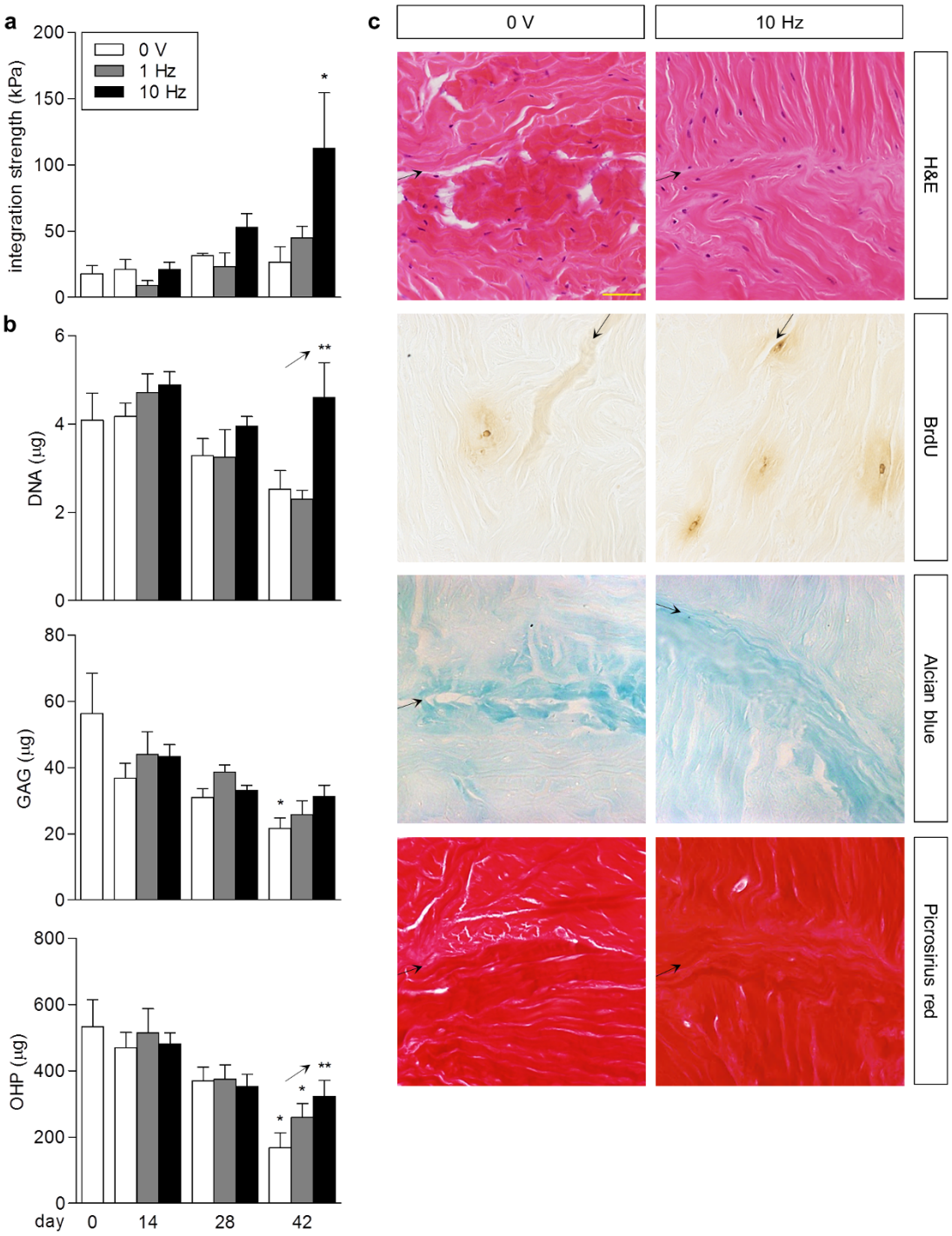

Figure 4 | Electrical stimulation enhanced integrative repair and maintained the biochemical composition of explants. (a) Integration strength of full-thickness defects in meniscus explants over six weeks with (3 V/cm, 1 Hz, 2 ms or 3 V/cm, 10 Hz, 0.2 ms pulse duration) and without stimulation (0 V). By day 42, stimulation at 10 Hz significantly promoted integrative repair versus explants without stimulation (0 V) and stimulated at 1 Hz. * $p < 0.05$ vs. day 0, vs. 0 V and 1 Hz at day 42; $n = 3$–9. (b) Biochemical composition of meniscus explants over six weeks: total DNA, sulfated GAG, hydroxyproline (OHP). At day 42, stimulation corresponded to significant upward trends in DNA and OHP content of explants compared to controls (0 V). Stimulation at 10 Hz maintained GAG and OHP content relative to day 0, in comparison to no stimulation (0 V) and stimulation at 1 Hz. * $p < 0.05$ vs. day 0; ** $p < 0.04$ for linear trend; $n = 3$–9. (c) Histological staining of meniscus explants at day 42: H&E for cell nuclei and cytoplasmic elements, BrdU for proliferating cells, Alcian blue for sulfated GAGs, Picrosirius red for collagens. The interface at the site of injury (arrows) appeared closely apposed with cells and newly synthesized matrix in explants stimulated at 10 Hz compared to no stimulation (0 V). Stimulated explants stained moderately more positive for BrdU+ nuclei, suggestive of enhanced cellular proliferation. Scale bar: 50 µm.

vitro. These changes in explants without stimulation occurred early in culture, within the first three weeks, but their biochemical composition continued to decrease for the remainder of the culture period.

Adenosine A_{2b} receptor plays a role in meniscus electrotransduction. Adenosine receptors in meniscus were identified by gene expression analysis of migrating cells, with and without stimulation at 3 V/cm, 10 Hz, 0.2 ms pulse duration. In hydrogel-encapsulated

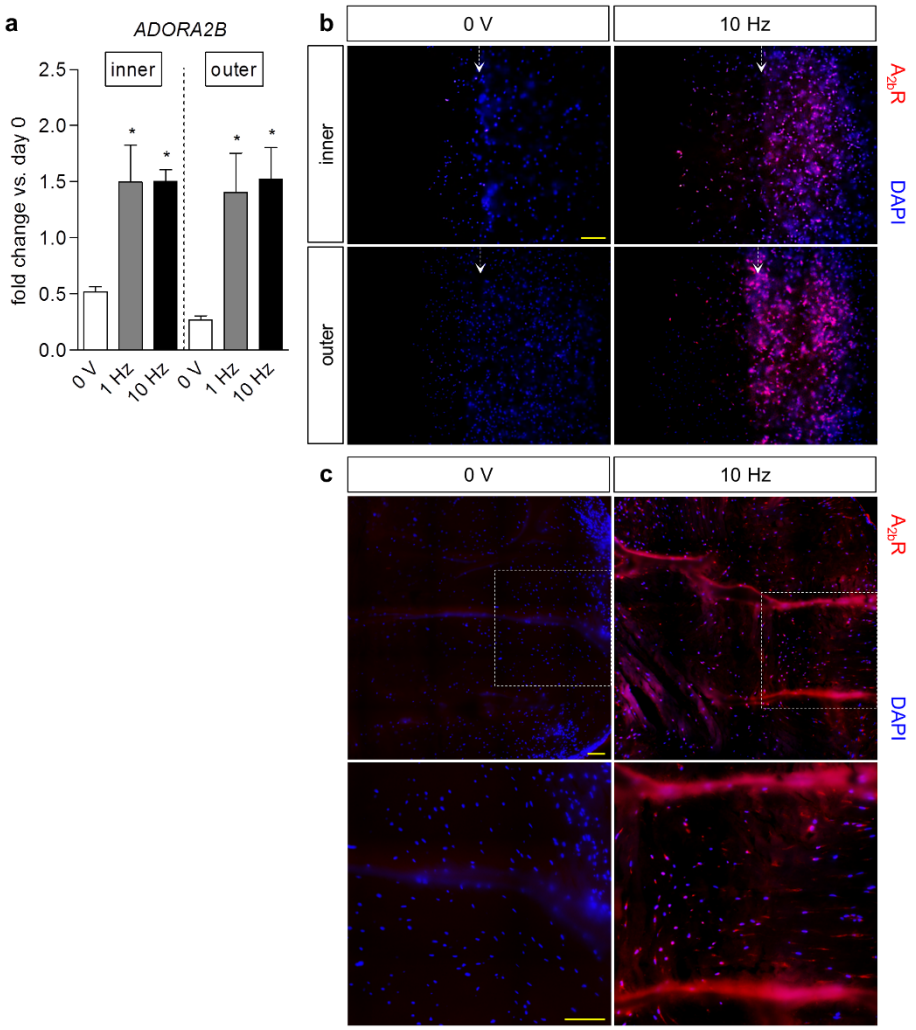

Figure 5 | Putative role of adenosine A_{2b} receptor in mediating electrical stimulation of meniscus. (a) Fold change ($2^{-\Delta\Delta C_T}$) in gene expression of *ADORA2B* in meniscus cells at day 6 relative to cells at day 0, respectively, both normalized to *GAPDH*. The addition of electrical stimulation (3 V/cm, 1 Hz, 2 ms or 3 V/cm, 10 Hz, 0.2 ms pulse duration) upregulated expression of the gene encoding the adenosine A_{2b} receptor ($A_{2b}R$). * $p < 0.05$ vs. 0 V; $n = 3$–4. (b) Immunofluorescence staining of migrating meniscus cells at day 6 with (3 V/cm, 10 Hz, 0.2 ms pulse duration) and without (0 V) stimulation, against $A_{2b}R$ and DAPI for nuclei. Stimulated cells exhibited positive staining for $A_{2b}R$, but not cells without stimulation. Arrows indicate the left edge of channels. Scale bar: 200 μm. (c) Immunofluorescence staining in meniscus explants at day 42 with (3 V/cm, 10 Hz, 0.2 ms pulse duration) and without electrical stimulation (0 V), of $A_{2b}R$ and nuclei. Cells in stimulated explants only exhibited positive staining for $A_{2b}R$. Boxes (top) indicate the areas pertaining to high magnification images (bottom). Scale bar: 50 μm.

cells, the expression of *ADORA1, ADORA2A*, and *ADORA3*, encoding the adenosine A_1, A_{2a}, and A_3 receptors, respectively, was minimal at day 0 ($2^{-\Delta C_T} \ll 10^{-4}$; $n = 4$) and at day 6 after culture, with and without stimulation ($2^{-\Delta C_T} \ll 10^{-5}$; $n = 4$), but *ADORA2B* encoding $A_{2b}R$ was upregulated in meniscus cells with electrical stimulation at 3 V/cm, 10 Hz, 0.2 ms, as well as 3 V/cm, 1 Hz, 0.2 ms pulse duration (Fig. 5a). Translation to the protein level was evident through immunofluorescence staining of migrating meniscus cells at day 6, against $A_{2b}R$ and DAPI for nuclei (Fig. 5b). Cells receiving stimulation demonstrated strong, positive staining for $A_{2b}R$, while cells without stimulation exhibited little or none, suggesting that the applied electrical signals may activate $A_{2b}R$ directly.

At the macro-scale level, cells in stimulated explants also stained positively for $A_{2b}R$, whereas those not receiving stimulation appeared negative (Fig. 5c), lending further evidence to the potential relationship between electrical signals and activation of the adenosine A_{2b} receptors in meniscus. Moreover, the consistency in protein expression from the micro- to macro-scale continues to support the use of micro-scale systems for evaluation of a broad range of electrical stimulation regimes, in order to identify the optimal parameters to apply at the macro-scale tissue level.

Discussion

Electrical stimulation is a versatile treatment modality that has yet to be fully explored in the context of injuries to the meniscus, in which negatively charged glycosaminoglycans form the basis for endogenous electrical activity[26,29,30]. We demonstrate that pulsatile direct current electric fields enhance meniscus cell migration in a micropatterned hydrogel system, and the integrative repair of meniscus defects in an *in vitro* explant model of meniscus healing. Notably, the responses of meniscus cells from the inner and outer regions were comparable, suggesting that the meniscus cells from both regions can be induced to migrate and promote healing by external electrical signals.

In our 3-D systems, electrical stimulation alone induced similar migration behavior in cells isolated from both the inner and outer regions, whereas previous studies have shown that outer cells migrate more quickly than inner cells during 2-D galvanotaxis[42]. This

disparity in observation may arise in part from the use of distinct cell populations within the meniscus between the two studies: cells isolated by tissue explant outgrowth in culture in the present study, versus cells isolated by release from tissue matrix via digestion in the galvanotaxis studies[42]. The inner and outer meniscus cells used in our study were previously characterized as a population capable of differentiating along multiple lineages, and may represent tissue-specific stem cells contributing to endogenous repair[51]. These cells, by nature of their isolation via tissue outgrowth, exhibit a predisposition for migration, which may also account for the level of motility observed in cells, even in the absence of electrical stimulation. As such, an enriched population of these cells after passaging may have led to a more robust response to exogenous electrical stimuli than a mixed population obtained by digestion in previous studies. In addition, the applied electric fields in the current study were perpendicular to the direction of cell migration, but no bias in polarity of movement was observed, in contrast to the cathodal migration of meniscus cells during 2-D galvanotaxis[42]. However, the observed behavior is consistent with studies of human fibroblasts on 3-D collagen gels in static DC fields, in which preferred movement occurred perpendicular to the axis of stimulation, but not towards a specific pole[43].

The fibrin hydrogel used in the micropatterned system represented a simple three-dimensional environment to observe meniscus cell migration phenomena. However, it does not begin to replicate the dense tissue matrix found in the native meniscus. Therefore, it was particularly encouraging to discover that the parameters optimized at the hydrogel level were applicable at the tissue level, inducing the migration of endogenous repair cells to the defect interface. However, migration at the tissue level also necessarily requires remodeling of the dense surrounding matrix to enable movement, which involves the interplay and balance of pro-inflammatory cytokines and MMPs, and anti-inflammatory and anabolic factors. After meniscus injury, experimentally induced or clinically occurring, this balance is tilted in favor of pro-inflammatory, catabolic events, necessitating examination into interventions that can re-initiate synthesis of key ECM components. It has been previously reported that meniscus explants lose their biochemical properties, specifically, DNA[49] and GAG[49,50] content, over time in culture. In this study, a similar loss in DNA and GAG content was seen in explants without stimulation over six weeks, and in addition, we observed a significant loss of collagen content. Interestingly, the explants receiving the optimal stimulation regime maintained their biochemical composition, suggesting a stabilizing effect of electrical stimulation, moving the balance away from the destructive aspect of remodeling towards the constructive side. By applying the findings on the cellular micro-scale to the tissue macro-scale, an additional benefit of electrical stimulation was revealed, that it may counteract the natural degradation of explant tissue *in vitro*, in addition to mediating cell migration.

In order to understand the basis of the *in vitro* degradation, the concentration of pro-inflammatory cytokines, TNF-α and IL-1β, were measured in the media collected during explant culture. The fetal bovine serum used in culture medium contained baseline amounts of both cytokines, but it is notable that statistically significant differences existed between the levels of TNF-α and IL-1β in explant culture media, with and without stimulation, in the absence of exogenous supplementation of either cytokine or other pro-inflammatory mediators. In clinical observation, synovial fluid from patients who underwent arthroscopy for a meniscus tear contained between 35–85 pg/mL TNF-α, and 90–125 pg/mL IL-1β[52]. The level of TNF-α detected in this system was well above what was found in a pathological state of meniscus injury, but within the working range of exogenous supplementation in other studies of meniscus repair[20]. In contrast, IL-1β was below both pathologic levels and the range used in other meniscus studies[53]. IL-1α levels were not measured in this study, but are relevant due to the differences in relative potency of IL-1α and β in porcine meniscus explants[54]. Moreover, the effects of TNF-α and IL-1 were not independent, and interplay between the two cytokines in activating pro-inflammatory pathways has been documented[14–19]. The lower levels of TNF-α and IL-1β in explants receiving the optimal stimulation regime suggest inhibitory effects of electrical stimulation on their production. In contrast, increases in these cytokines were observed in explants without stimulation, with corresponding increases in NO production, MMP activity, and subsequent GAG loss in media. These two observations correlate with previous findings demonstrating that inhibition of MMPs can significantly reduce GAG loss in culture[50]. The loss of explant stability in the absence of electrical stimulation, particularly in the first half of the culture period, corresponds with the observation that meniscus injury disrupts tissue homeostasis and initiates a series of events furthering degradation[8,55–57].

The migration and anti-inflammatory responses elicited by electrical stimulation occur via the activation of membrane receptors on meniscus cells. It has been previously postulated that electromagnetic fields can serve as first messengers in signaling towards tissue repair[58]. Based upon the findings in this study, a new model of electrotransduction in meniscus could be proposed: after meniscus injury, TNF-α and IL-1 levels are elevated, progressing toward further tissue degradation (Fig. 6a). Within this environment, the application of pulsatile DC electrical stimulation selectively activates the adenosine A_{2b} receptor, producing the second messenger cAMP, which triggers anti-inflammatory pathways that reduce NO production, MMP activity, and GAG release, and inhibit the initial pro-inflammatory cytokines (Fig. 6b).

The physiological role of low-affinity $A_{2b}R$ has been less characterized than the high-affinity $A_{2a}R$, which has been studied extensively for anti-inflammatory activity in the context of osteoarthritis and rheumatoid arthritis[59–61]. However, activation of the $A_{2b}R$, leading to elevated cAMP, has been shown to inhibit MMP-1 production in fibroblast-like synoviocytes from RA patients[62], and in this study, we report for the first time in meniscus, among the class of adenosine receptors, the increased expression of $A_{2b}R$ following electrical stimulation at both the micro- and macro-scale. In order to fully elucidate the role of $A_{2b}R$ in meniscus electrotransduction, further experiments using receptor agonists and antagonists must be tested in meniscus defect models, with the addition of exogenous sources of pro-inflammatory cytokines to the system, and measurement of changes in adenylyl cyclase and cAMP levels. To this end, our micro-scale system for meniscus cell migration will allow for blocking or knock-down of the adenosine A_{2b} receptor by antagonists or gene silencing, in order to verify the integral role of $A_{2b}R$ via short-term experiments, and subsequent application at the macro-scale in long-term culture of explants, for confirmation at the tissue level. Moreover, cells and explants in this study were derived from juvenile bovine meniscus, requiring future studies using adult or even osteoarthritic tissue to confirm and extend findings. While growth factors were not supplemented to medium in this system, the addition of TGF-β3 alone[49] or TGF-β1 in the presence of IL-1[63] has been shown to significantly enhance meniscus repair, meriting the further study of any potential synergy between electrical and chemical stimuli. However, it should be noted that the reparative and protective effects of electrical stimulation alone, as shown in this study, are more immediately translatable to the clinic, without the need for *in vivo* delivery of growth factors. Moreover, the integration strength of explants stimulated at the optimal regime is among the highest reported in literature for this model of meniscal repair, even in the absence of exogenous growth factors[20–22,49,63,64].

The contribution of growth factors was explored at the micro-scale through the co-culture of endothelial cells, as a model of clinical methods that increase the vascular response to the inner region[65,66], which does not naturally undergo repair. Although up to 30% of

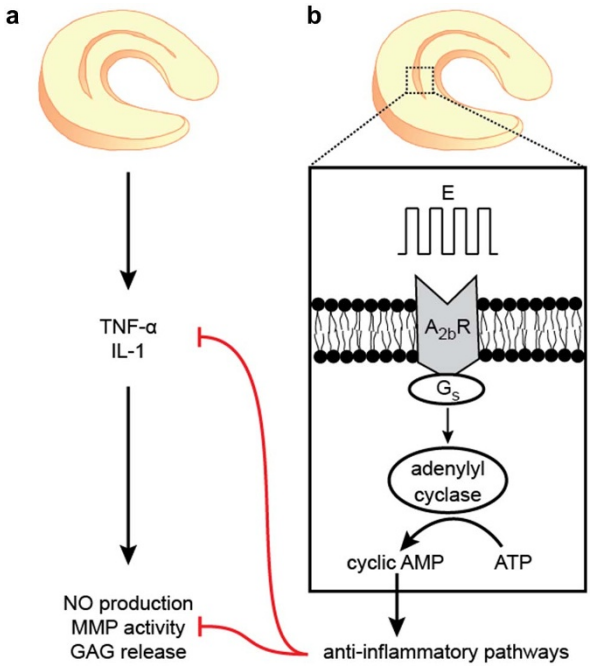

Figure 6 | Proposed model of meniscus electrotransduction. (a) After meniscus injury, elevated levels of the pro-inflammatory cytokines, TNF-α and IL-1, lead to increases in nitric oxide (NO) production, matrix metalloproteinase (MMP) activity, GAG release, and overall tissue degradation. (b) Transduction of pulsatile direct current electrical signals (E) may occur by G protein-coupled adenosine A_{2b} receptors on the meniscus cell membrane, which stimulate adenylyl cyclase via G_s and activate cyclic AMP. Increases in intracellular cAMP trigger anti-inflammatory pathways, which suppress NO production, MMP activity, and GAG release, and inhibit the initial cytokines. These downstream effects may prevent the degradation of meniscus tissue that leads to osteoarthritis.

the meniscus is vascularized in adults[67], and endothelial cells from the meniscus have been isolated and cultured[68], the exact percentage of endothelial cells in the tissue remains unknown. However, endothelial cells may potentiate their effects via paracrine signaling, and these angiogenic factors can be supplemented in avascular tissues where they and endothelial cells are natively absent, such as in the inner region of the meniscus. Here we report that the combination of biophysical and biochemical stimuli via EFs and co-culture with HUVECs cooperatively enhanced the migration of meniscus cells in a 3-D environment. Despite the variation in vascularity of their respective tissue regions, inner and outer cells demonstrated trends of increased migration in the presence of both stimuli as compared to either stimulus alone. The cooperative effects of electrical signals and HUVECs appeared to result from the direct effects of electrical signals on HUVECs, which have been shown to regulate HUVEC behavior[46], and in our system, upregulated the gene expression of angiogenic factors such as endothelin-1 and PDGF isoforms, previously shown to act on chondrocytes[47] and meniscus cells[48]. Curiously, we observed a regional variation in expression of endothelin and PDGF receptors by meniscus cells in co-culture with HUVECs, which is now the focus of ongoing studies to examine the differential paracrine mechanisms of endothelial cells on the meniscus. Specifically, we will investigate if direct interactions between meniscus and endothelial cells are necessary, or if paracrine factors secreted by endothelial cells are sufficient to induce migration behavior in outer cells, which natively co-exist with vasculature, versus inner cells, which do not. The differential expression of PDGF receptor genes in outer versus inner cells in co-culture with HUVECs may arise from the presence of endothelial cells in one region versus the other, a disparity that was further amplified by electrical signals. However, the upregulation of ET_AR gene expression in cells of both regions with co-culture suggests that ET-1 signaling is involved in the vascular response of the outer region for healing. Moreover, the limited healing potential of the inner region could be enhanced if ET-1 is supplemented to the avascular tissue, which does not receive these signals natively in the absence of endothelial cells. If these differential paracrine mechanisms of HUVECs on cells from the inner and outer regions are validated in future studies, by applying conditioned medium or specific angiogenic factors, we not only gain a further understanding of the variation in repair response between the two regions, but we also identify the angiogenic factors that are natively absent in the inner region, but can be supplemented in order to promote healing.

In addition, we found that the coordinated action of EFs and HUVECs on meniscus cell migration was more apparent using a different set of stimulation parameters than for EFs alone. This observation, as well as the variation in migration response seen during initial optimization of parameters for meniscus cells only, is in line with previous theories that a window exists in which productive electrical stimulation occurs[33], and parameters must be optimized for all relevant cell types within the system. Moreover, although the co-culture studies were performed at one fixed channel-to-channel distance, the system can be easily modified to vary this distance by simply changing the design of the micropattern, in order to identify a length scale over which paracrine signaling occurs. Although it was not tested in this study, the interaction of electrical stimulation and endothelial cells is pertinent at the tissue level as well, with implications for clinical and adjuvant therapies. However, *in vitro* models of meniscus repair cannot fully replicate the regional variation in vascular environment within the tissue and its influence on healing[64]. Experimentation in an animal model is the most suitable next step towards validation of electrical stimulation as a modality for treatment of meniscus injury.

In summary, the effects of pulsatile electric field stimulation on meniscus repair were demonstrated for the first time. Optimization of electrical stimulation regimes for cell migration was achieved at the micro-scale with short-term experiments, and then applied at the macro-scale towards significant integrative repair of full-thickness defects in meniscus explants. *In situ* stimulation of explants revealed another role of electric fields in modulating inflammation and reducing tissue degradation. The dual functions of electrical stimulation in meniscus support its use in the clinical setting, after surgical intervention, to recruit cells for tissue repair and to prevent the matrix degradation that leads to osteoarthritis. Future establishment of therapeutic strategies, by testing stimulation regimes and translating to macro-scale tissue repair, has the potential to overcome current limitations in meniscus healing.

Methods

Cell isolation. Juvenile bovine meniscus cells were isolated from the inner and outer regions as previously described[51]. Briefly, the menisci of calves were obtained from a commercial source (Green Village Packing Company), dissected within 36 h of slaughter, and sectioned into inner (2/3) and outer (1/3) regions. The tissue was then minced into 1–2 mm^3 pieces, and plated on tissue culture plates in basal medium consisting of high glucose DMEM, 1× antibiotic-antimycotic, 10% FBS, and 50 μg/mL ascorbate 2-phosphate. Over 2–3 weeks, cells migrated out of the tissue pieces, and were expanded to passage 2.

Human umbilical vein endothelial cells (HUVECs) were isolated from fresh umbilical cords of term delivery, collected according to an active IRB at Columbia University (IRB-AAAC4839)[69]. According to the protocol, tissue samples were fully deidentified and there was no patient information available to the investigators. Umbilical cords were rinsed with PBS, and the umbilical vein lumen was infused with a 2.5% trypsin solution and clamped at both ends. Enzymatic digestion occurred at 37°C for 15 min, and the resulting cell digest was collected by rinsing the vein with PBS and centrifugation at 300 × g for 5 min. The cell pellet was resuspended on 25 cm^2 tissue culture flasks in endothelial growth medium (EGM-2, Lonza), and expanded to passage 5.

Explant culture. Juvenile bovine meniscus explants were harvested from the central tissue region using sterile 4 mm Ø biopsy punches, and cut to 1.5 mm height using a custom microtome device. A 1.5 mm Ø central core was punched and immediately replaced into the explant ring to simulate a full-thickness defect. Explants were cultured for 3 days in basal medium prior to the start of each experiment.

Cell migration assay. The micropatterned three-dimensional hydrogel system used in cell migration studies was previously established for the study of human mesenchymal stem cells and HUVECs in co-culture[69]. Briefly, the poly(dimethylsiloxane) (PDMS; 9 : 1 elastomer:curing agent; Sylgard 184 silicone elastomer kit, Dow Corning) micropattern consisted of two parallel channels (1 cm length, 1000 μm width, 200 μm height, channel-to-channel distance: 2000 μm; Fig. 1b). Prior to cell encapsulation, the PDMS surface was blocked using a 5% solution of FBS in sterile distilled water.

In single channel studies (Fig. 1a), inner or outer meniscus cells were encapsulated at 3.5×10^6 cells/mL each in 1.8% fibrin (bovine fibrinogen, MP Biomedicals; thrombin from bovine plasma, Sigma-Aldrich) and printed into single channels on plastic slides. The cell-fibrin suspension was allowed to polymerize for 15 min, before removal of the PDMS mold and encapsulation in an additional layer of 1.8% fibrin to permit cell migration. In co-culture studies (Fig. 1b), inner or outer meniscus cells and HUVECs were encapsulated at 3.5×10^6 cells/mL each in 1.8% fibrin, printed into two parallel channels on plastic slides, and covered by another layer of 1.8% fibrin. Single channels of inner or outer meniscus cells served as controls. Cultures were maintained in EGM-2 over 6 days after encapsulation, and migration was monitored by bright field imaging at days 0 and 6, using an Olympus IX81 microscope with an IX2-UCB digital camera and Metamorph software.

Electrical stimulation of cells. After 3 days of pre-culture without stimulation, the cells were transferred into custom bioreactors with carbon electrodes (Ladd Research Industries) spaced 2.5 cm apart (Fig. 1a)[70]. Bioreactors were connected by platinum wire to an electrical stimulator (Grass Technologies) generating continuous pulses of 7.5 V, corresponding to a field strength of 3 V/cm, and various frequency and pulse duration combinations (0.1, 1, 10 Hz and 2 ms pulse duration; 10 Hz and 0.2 ms pulse duration) for 3 days. Bioreactors not connected to the stimulator served as controls (0 V).

Electrical stimulation of explants. After 3 days of pre-culture, explants were stimulated in a custom bioreactor (Fig. 1c), consisting of a 5×6 array outfitted with carbon electrodes that were spaced 1 cm apart, and connected directly to a stimulator generating pulses of 3 V, corresponding to a field strength of 3 V/cm, and either 1 Hz and 2 ms pulse duration or 10 Hz and 0.2 ms pulse duration. Each row was independently stimulated, with six wells per row receiving the same stimulation regime. Rows not connected to the stimulator served as controls (0 V). Explants were stimulated four days a week over six weeks of culture in basal medium, with media collection at each change, and sample collection for mechanical integration testing, biochemical assays, and histological and immunofluorescence staining at biweekly time points.

Evaluation of meniscus cell migration. Bright field images were processed using a custom MATLAB program[71] to track cell migration. Briefly, the program applied the Sobel edge detection algorithm and eliminated small regions of isolated, single meniscus cells. Each image was evenly subdivided into regions corresponding to ~1580 μm of the channel length, for which average channel-to-channel distances were calculated.

Real-time PCR. The total RNA of meniscus cells or HUVECs after six days of culture was extracted by TRIzol reagent (Invitrogen) and reverse transcribed (High Capacity cDNA Reverse Transcription Kit, Applied Biosystems). Meniscus cells and HUVECs were also collected at day 0 prior to encapsulation and processed to facilitate fold change analysis ($2^{-\Delta\Delta C_T}$). Real-time PCR was performed on an Applied Biosystems StepOnePlus Real-Time PCR System using Fast SYBR Green Master Mix (Invitrogen), custom bovine primers for *COL1A2, EDNRA, PDGFRA, PDGFRB, ADORA1, ADORA2A, ADORA2B, ADORA3*, and *GAPDH*, and custom human primers for *EDN1, PDGFA, PDGFB*, and *GAPDH*.

Mechanical integration testing of explants. The integration of full-thickness defects in explants was tested with a custom device consisting of a 1.33 mm Ø indenter in series with a 50 g load cell, placed above a cup with a 2 mm Ø hole. Prior to testing, the height of each sample was measured using a digital caliper. The indenter was displaced at a ramp rate of 0.3% of the sample height per second, until the central core was pushed fully through the outer ring. Integration strength was calculated as the ratio of the peak force to the surface area of contact between the central core and outer ring. After testing, samples were collected for further biochemical analysis.

Biochemical analysis of explants and media. The biochemical composition of explants was evaluated for DNA, sulfated GAG, and OHP content. Briefly, samples were lyophilized for 24 h and digested at 60°C for 16 h in a papain solution containing 125 μg/mL papain (Sigma-Aldrich), 50 mmol phosphate buffer (pH 6.5), and 2 mmol N-acetyl cysteine (Sigma-Aldrich). DNA content of the sample digests was obtained using the PicoGreen dsDNA quantitation kit (Invitrogen), according to manufacturer's protocol. Sulfated GAG content was measured using the 1,9-dimethylmethylene blue dye-binding (DMMB) assay[72]. Hydroxyproline (OHP) content was quantified by a modified acid hydrolysis assay[73]. Media collected at each change was assayed for TNF-α, IL-1β, and NO production, MMP activity, and GAG release using the DMMB assay. Briefly, TNF-α and IL-1β production were quantified directly on media samples using the bovine TNF-α (GenWay Biotech) and IL-1β (Thermo Fisher Scientific) ELISA kits, respectively. Prior to NO analysis, media samples were filtered through Vivaspin 500 units (10,000 MWCO PES filters, Sartorius), and total NO production in media samples was determined by quantification of nitrate and nitrite, according to manufacturer's protocol (nitrate/nitrite colorimetric assay kit, Cayman Chemical Company). The activity of MMP-1, -2, -3, -9, -13, and -14 was assessed via cleavage of a fluorescent peptide substrate (PEPDAB008, BioZyme), adapted from a previously published protocol[53]. Media samples were incubated in either 2.5 mM p-aminophenylmercuric acetate (APMA; pH 7.0–7.5) in assay buffer (200 mM NaCl, 50 mM Tris, 5 mM $CaCl_2$, 10 μM $ZnSO_4$, 0.01% Brij 35, pH 7.5) or in assay buffer alone at 37°C for 5 h. Samples were then diluted twofold with assay buffer containing 20 μM substrate at 37°C for 2 h, and measured at 485 nm excitation and 530 nm emission. Total MMP activity was calculated as the difference in fluorescence readings between samples incubated with and without APMA.

5-bromo-2-deoxyuridine labeling of cells and explants. At the endpoint of both migration and integration studies, samples were labeled with 5-bromo-2-deoxyuridine (BrdU, Invitrogen) to assess cellular proliferation. Single channel studies of meniscus cells were incubated with BrdU labeling reagent (1 : 50) at 37°C for 4 h, and explants (1 : 50) at 37°C overnight. Samples were then fixed for further histological processing.

Histological and immunofluorescence staining of cells and explants. Cell migration samples were fixed in a graded series of formaldehyde from 1% to 4% for 10 min each, and maintained in PBS at 4°C until preparation for staining. Briefly, samples were blocked and permeabilized with agitation in PBS containing 5% BSA and 0.1% Triton X-100 at 25°C for 1 h, and incubated at 4°C overnight with the primary antibody (rabbit anti-adenosine A_{2b} receptor antibody, 50 μg/mL, Millipore) in PBS with 5% BSA. After 3 washes of 30 min each in PBS at 25°C with agitation, samples were incubated at 4°C overnight with Alexa Fluor® 555 goat anti-rabbit IgG (1 : 200, Invitrogen) and DAPI (1 : 200, Invitrogen), followed by 3 additional washes. Alternatively, samples were directly incubated after blocking and permeabilization with DAPI and mouse anti-BrdU antibody (Alexa Fluor® 488 conjugate, 1 : 50, Invitrogen).

Explants were fixed in 4% formaldehyde at 4°C overnight and embedded in 2% low-melting-temperature agarose. All samples were dehydrated in a graded series of ethanol, embedded in paraffin, and sectioned to 8 μm thickness. Sections were stained with hematoxylin and eosin (H&E) for nuclei and cytoplasmic elements, respectively, Alcian blue (pH 1.0) for sulfated GAGs, and Picrosirius red for collagens. For immunofluorescence staining of $A_{2b}R$ in paraffin-embedded samples, antigen retrieval was performed with 10 mM citrate buffer (pH 6.0). Blocking in PBS with 5% BSA, and primary and secondary antibody incubations in PBS with 5% BSA were completed, as previously described. Immunohistochemical staining of BrdU was conducted, according to manufacturer's protocol (BrdU staining kit, Invitrogen). Stained hydrogels and explants were imaged with an Olympus FSX100 microscope.

Statistical analysis. For cell migration studies, 1-way ANOVA with Tukey post tests or post tests for linear trend were performed with Prism ($\alpha = 0.05$). For integration studies, 2-way ANOVA with Bonferroni post tests and 1-way ANOVA with post tests for linear trend were also performed with Prism. All data are presented as mean ± SEM.

1. Levin, M. Bioelectromagnetics in morphogenesis. *Bioelectromagnetics* **24**, 295–315 (2003).
2. Nuccitelli, R. Ionic currents in morphogenesis. *Experientia* **44**, 657–66 (1988).
3. Robinson, K. R. & Messerli, M. A. Left/right, up/down: the role of endogenous electrical fields as directional signals in development, repair and invasion. *Bioessays* **25**, 759–66 (2003).
4. Baker, B., Becker, R. O. & Spadaro, J. A study of electrochemical enhancement of articular cartilage repair. *Clin. Orthop. Relat. Res.* **102**, 251–67 (1974).
5. Baker, B., Spadaro, J., Marino, A. & Becker, R. O. Electrical stimulation of articular cartilage regeneration. *Ann. N. Y. Acad. Sci.* **238**, 491–9 (1974).
6. Lippiello, L., Chakkalakal, D. & Connolly, J. F. Pulsing direct current-induced repair of articular cartilage in rabbit osteochondral defects. *J. Orthop. Res.* **8**, 266–75 (1990).
7. Garrett, W. E. *et al.* American Board of Orthopaedic Surgery Practice of the Orthopaedic Surgeon: Part-II, certification examination case mix. *J. Bone Joint Surg. Am.* **88**, 660–7 (2006).
8. Higuchi, H., Kimura, M., Shirakura, K., Terauchi, M. & Takagishi, K. Factors affecting long-term results after arthroscopic partial meniscectomy. *Clin. Orthop. Relat. Res.* **377**, 161–8 (2000).
9. Arnoczky, S. P. & Warren, R. F. The microvasculature of the meniscus and its response to injury. An experimental study in the dog. *Am. J. Sports Med.* **11**, 131–41 (1983).
10. Cheung, H. S. Distribution of type I, II, III and V in the pepsin solubilized collagens in bovine menisci. *Connect. Tissue Res.* **16**, 343–56 (1987).

11. Sweigart, M. A. & Athanasiou, K. A. Toward tissue engineering of the knee meniscus. *Tissue Eng.* **7**, 111–29 (2001).
12. Hardingham, T. E. & Fosang, A. J. Proteoglycans: many forms and many functions. *FASEB J.* **6**, 861–70 (1992).
13. Lohmander, L. S., Dahlberg, L., Ryd, L. & Heinegård, D. Increased levels of proteoglycan fragments in knee joint fluid after injury. *Arthritis Rheum.* **32**, 1434–42 (1989).
14. Lotz, M. Cytokines in cartilage injury and repair. *Clin. Orthop. Relat. Res.* **391**, S108–15 (2001).
15. Fernandes, J. C., Martel-Pelletier, J. & Pelletier, J.-P. The role of cytokines in osteoarthritis pathophysiology. *Biorheology* **39**, 237–46 (2002).
16. Lotz, M. *et al*. Cytokine regulation of chondrocyte functions. *J. Rheumatol. Suppl.* **43**, 104–8 (1995).
17. LeGrand, A. *et al*. Interleukin-1, tumor necrosis factor alpha, and interleukin-17 synergistically up-regulate nitric oxide and prostaglandin E2 production in explants of human osteoarthritic knee menisci. *Arthritis Rheum.* **44**, 2078–83 (2001).
18. Shin, S.-J., Fermor, B., Weinberg, J. B., Pisetsky, D. S. & Guilak, F. Regulation of matrix turnover in meniscal explants: role of mechanical stress, interleukin-1, and nitric oxide. *J. Appl. Physiol.* **95**, 308–13 (2003).
19. Fermor, B. *et al*. The effects of cyclic mechanical strain and tumor necrosis factor alpha on the response of cells of the meniscus. *Osteoarthritis Cartilage* **12**, 956–62 (2004).
20. McNulty, A. L., Moutos, F. T., Weinberg, J. B. & Guilak, F. Enhanced integrative repair of the porcine meniscus in vitro by inhibition of interleukin-1 or tumor necrosis factor alpha. *Arthritis Rheum.* **56**, 3033–42 (2007).
21. Wilusz, R. E., Weinberg, J. B., Guilak, F. & McNulty, A. L. Inhibition of integrative repair of the meniscus following acute exposure to interleukin-1 in vitro. *J. Orthop. Res.* **26**, 504–12 (2008).
22. McNulty, A. L., Estes, B. T., Wilusz, R. E., Weinberg, J. B. & Guilak, F. Dynamic loading enhances integrative meniscal repair in the presence of interleukin-1. *Osteoarthritis Cartilage* **18**, 830–8 (2010).
23. Gu, W. Y., Lai, W. M. & Mow, V. C. Transport of fluid and ions through a porous-permeable charged-hydrated tissue, and streaming potential data on normal bovine articular cartilage. *J. Biomech.* **26**, 709–23 (1993).
24. Gu, W. Y., Lai, W. M. & Mow, V. C. A mixture theory for charged-hydrated soft tissues containing multi-electrolytes: passive transport and swelling behaviors. *J Biomech Eng* **120**, 169–180 (1998).
25. Lai, W. M., Mow, V. C., Sun, D. D. & Ateshian, G. A. On the electric potentials inside a charged soft hydrated biological tissue: streaming potential versus diffusion potential. *J. Biomech. Eng.* **122**, 336–46 (2000).
26. Grodzinsky, A. J., Lipshitz, H. & Glimcher, M. J. Electromechanical properties of articular cartilage during compression and stress relaxation. *Nature* **275**, 448–50 (1978).
27. Schmidt-Rohlfing, B., Schneider, U., Goost, H. & Silny, J. Mechanically induced electrical potentials of articular cartilage. *J. Biomech.* **35**, 475–82 (2002).
28. Bassett, C. A. & Pawluk, R. J. Electrical behavior of cartilage during loading. *Science* **178**, 982–3 (1972).
29. Frank, E. H. & Grodzinsky, A. J. Cartilage electromechanics–II. A continuum model of cartilage electrokinetics and correlation with experiments. *J. Biomech.* **20**, 629–639 (1987).
30. Mow, V. C., Wang, C. C. & Hung, C. T. The extracellular matrix, interstitial fluid and ions as a mechanical signal transducer in articular cartilage. *Osteoarthritis Cartilage* **7**, 41–58 (1999).
31. Brighton, C. T., Jensen, L., Pollack, S. R., Tolin, B. S. & Clark, C. C. Proliferative and synthetic response of bovine growth plate chondrocytes to various capacitively coupled electrical fields. *J. Orthop. Res.* **7**, 759–65 (1989).
32. Rodan, G. A., Bourret, L. A. & Norton, L. A. DNA synthesis in cartilage cells is stimulated by oscillating electric fields. *Science* **199**, 690–2 (1978).
33. Armstrong, P. F., Brighton, C. T. & Star, A. M. Capacitively coupled electrical stimulation of bovine growth plate chondrocytes grown in pellet form. *J. Orthop. Res.* **6**, 265–71 (1988).
34. Brighton, C. T., Unger, A. S. & Stambough, J. L. In vitro growth of bovine articular cartilage chondrocytes in various capacitively coupled electrical fields. *J. Orthop. Res.* **2**, 15–22 (1984).
35. Wang, W., Wang, Z., Zhang, G., Clark, C. C. & Brighton, C. T. Up-regulation of chondrocyte matrix genes and products by electric fields. *Clin. Orthop. Relat. Res.* **427**, S163–73 (2004).
36. Ciombor, D. M., Aaron, R. K., Wang, S. & Simon, B. Modification of osteoarthritis by pulsed electromagnetic field--a morphological study. *Osteoarthritis Cartilage* **11**, 455–62 (2003).
37. Ongaro, A. *et al*. Electromagnetic fields (EMFs) and adenosine receptors modulate prostaglandin E(2) and cytokine release in human osteoarthritic synovial fibroblasts. *J. Cell. Physiol.* **227**, 2461–9 (2012).
38. De Mattei, M. *et al*. Adenosine analogs and electromagnetic fields inhibit prostaglandin E2 release in bovine synovial fibroblasts. *Osteoarthritis Cartilage* **17**, 252–62 (2009).
39. Haskó, G., Linden, J., Cronstein, B. & Pacher, P. Adenosine receptors: therapeutic aspects for inflammatory and immune diseases. *Nat. Rev. Drug Discov.* **7**, 759–70 (2008).
40. Mediero, A. & Cronstein, B. N. Adenosine and bone metabolism. *Trends Endocrinol. Metab.* **24**, 290–300 (2013).
41. Fini, M. *et al*. Functional tissue engineering in articular cartilage repair: is there a role for electromagnetic biophysical stimulation? *Tissue Eng. Part B. Rev.* **19**, 353–67 (2013).
42. Gunja, N. J. *et al*. Migration responses of outer and inner meniscus cells to applied direct current electric fields. *J. Orthop. Res.* **30**, 103–11 (2012).
43. Sun, S., Wise, J. & Cho, M. Human fibroblast migration in three-dimensional collagen gel in response to noninvasive electrical stimulus. I. Characterization of induced three-dimensional cell movement. *Tissue Eng.* **10**, 1548–57 (2004).
44. Mont, M. A. *et al*. Pulsed electrical stimulation to defer TKA in patients with knee osteoarthritis. *Orthopedics* **29**, 887–92 (2006).
45. Farr, J., Mont, M. A., Garland, D., Caldwell, J. R. & Zizic, T. M. Pulsed electrical stimulation in patients with osteoarthritis of the knee: follow up in 288 patients who had failed non-operative therapy. *Surg. Technol. Int.* **15**, 227–33 (2006).
46. Zhao, M., Bai, H., Wang, E., Forrester, J. V. & McCaig, C. D. Electrical stimulation directly induces pre-angiogenic responses in vascular endothelial cells by signaling through VEGF receptors. *J. Cell Sci.* **117**, 397–405 (2004).
47. Khatib, A. M. *et al*. Endothelin 1 receptors, signal transduction and effects on DNA and proteoglycan synthesis in rat articular chondrocytes. *Cytokine* **10**, 669–79 (1998).
48. Bhargava, M. M. *et al*. The effect of cytokines on the proliferation and migration of bovine meniscal cells. *Am. J. Sports Med.* **27**, 636–43 (1999).
49. Ionescu, L. C. *et al*. Maturation state-dependent alterations in meniscus integration: implications for scaffold design and tissue engineering. *Tissue Eng. Part A* **17**, 193–204 (2011).
50. Wilson, C. G., Vanderploeg, E. J., Zuo, F., Sandy, J. D. & Levenston, M. E. Aggrecanolysis and in vitro matrix degradation in the immature bovine meniscus: mechanisms and functional implications. *Arthritis Res. Ther.* **11**, R173 (2009).
51. Mauck, R. L., Martinez-Diaz, G. J., Yuan, X. & Tuan, R. S. Regional multilineage differentiation potential of meniscal fibrochondrocytes: implications for meniscus repair. *Anat. Rec. (Hoboken).* **290**, 48–58 (2007).
52. Vangsness, C. T., Burke, W. S., Narvy, S. J., MacPhee, R. D. & Fedenko, A. N. Human knee synovial fluid cytokines correlated with grade of knee osteoarthritis--a pilot study. *Bull. NYU Hosp. Jt. Dis.* **69**, 122–7 (2011).
53. McNulty, A. L., Miller, M. R., O'Connor, S. K. & Guilak, F. The effects of adipokines on cartilage and meniscus catabolism. *Connect. Tissue Res.* **52**, 523–33 (2011).
54. McNulty, A. L., Rothfusz, N. E., Leddy, H. a. & Guilak, F. Synovial fluid concentrations and relative potency of interleukin-1 alpha and beta in cartilage and meniscus degradation. *J. Orthop. Res.* **31**, 1039–45 (2013).
55. Andersson-Molina, H., Karlsson, H. & Rockborn, P. Arthroscopic partial and total meniscectomy: A long-term follow-up study with matched controls. *Arthroscopy* **18**, 183–9 (2002).
56. Englund, M., Roos, E. M. & Lohmander, L. S. Impact of type of meniscal tear on radiographic and symptomatic knee osteoarthritis: a sixteen-year followup of meniscectomy with matched controls. *Arthritis Rheum.* **48**, 2178–87 (2003).
57. McGinity, J. B., Geuss, L. F. & Marvin, R. A. Partial or total meniscectomy: a comparative analysis. *J. Bone Joint Surg. Am.* **59**, 763–6 (1977).
58. Pilla, A. *et al*. Electromagnetic fields as first messenger in biological signaling: Application to calmodulin-dependent signaling in tissue repair. *Biochim. Biophys. Acta* **1810**, 1236–45 (2011).
59. Flögel, U. *et al*. Selective activation of adenosine A2A receptors on immune cells by a CD73-dependent prodrug suppresses joint inflammation in experimental rheumatoid arthritis. *Sci. Transl. Med.* **4**, 146ra108 (2012).
60. Ralph, J. A. *et al*. Modulation of orphan nuclear receptor NURR1 expression by methotrexate in human inflammatory joint disease involves adenosine A2A receptor-mediated responses. *J. Immunol.* **175**, 555–65 (2005).
61. Ohta, A. & Sitkovsky, M. Role of G-protein-coupled adenosine receptors in downregulation of inflammation and protection from tissue damage. *Nature* **414**, 916–20.
62. Boyle, D. L., Sajjadi, F. G. & Firestein, G. S. Inhibition of synoviocyte collagenase gene expression by adenosine receptor stimulation. *Arthritis Rheum.* **39**, 923–30 (1996).
63. McNulty, A. L. & Guilak, F. Integrative repair of the meniscus: lessons from in vitro studies. *Biorheology* **45**, 487–500 (2008).
64. Hennerbichler, A., Moutos, F. T., Hennerbichler, D., Weinberg, J. B. & Guilak, F. Repair response of the inner and outer regions of the porcine meniscus in vitro. *Am. J. Sports Med.* **35**, 754–62 (2007).
65. Okuda, K., Ochi, M., Shu, N. & Uchio, Y. Meniscal rasping for repair of meniscal tear in the avascular zone. *Arthroscopy* **15**, 281–6 (1999).
66. Freedman, K. B., Nho, S. J. & Cole, B. J. Marrow stimulating technique to augment meniscus repair. *Arthroscopy* **19**, 794–8 (2003).
67. Greis, P. E., Bardana, D. D., Holmstrom, M. C. & Burks, R. T. Meniscal injury: I. Basic science and evaluation. *J Am Acad Orthop Surg* **10**, 168–176 (2002).
68. Miller, R. R. & Rydell, P. A. Primary culture of microvascular endothelial cells from canine meniscus. *J. Orthop. Res.* **11**, 907–11 (1993).
69. Trkov, S., Eng, G., Di Liddo, R., Parnigotto, P. P. & Vunjak-Novakovic, G. Micropatterned three-dimensional hydrogel system to study human endothelial-mesenchymal stem cell interactions. *J. Tissue Eng. Regen. Med.* **4**, 205–15 (2010).
70. Tandon, N. *et al*. Electrical stimulation systems for cardiac tissue engineering. *Nat. Protoc.* **4**, 155–73 (2009).

71. Chao, P.-H. G., Lu, H. H., Hung, C. T., Nicoll, S. B. & Bulinski, J. C. Effects of applied DC electric field on ligament fibroblast migration and wound healing. *Connect. Tissue Res.* **48**, 188–97 (2007).
72. Farndale, R. W., Buttle, D. J. & Barrett, A. J. Improved quantitation and discrimination of sulphated glycosaminoglycans by use of dimethylmethylene blue. *Biochim. Biophys. Acta* **883**, 173–7 (1986).
73. Reddy, G. K. & Enwemeka, C. S. A simplified method for the analysis of hydroxyproline in biological tissues. *Clin. Biochem.* **29**, 225–9 (1996).

Acknowledgments

We gratefully acknowledge NIH support of this work (grants EB002520, EB015888, DE016525, and AR061988). We also thank George Eng for his assistance with the micropatterned system, endothelial cell isolation, and bioreactor design; Kara Spiller for endothelial cell isolation; Keith Yeager for custom device design; Nina Tandon for bioreactor design; and Quentin Jallerat for his contribution to figures.

Author contributions

X.Y., P.G.C. and G.V.N. designed research; X.Y. and D.E.A. performed research; X.Y., D.E.A., P.G.C. and G.V.N. analyzed data; X.Y. and G.V.N. wrote the paper. All authors discussed the results and commented on the paper.

Additional information

Supplementary information accompanies this paper at http://www.nature.com/scientificreports

Competing financial interests: The authors declare no competing financial interests.

How to cite this article: Yuan, X., Arkonac, D.E., Chao, P.-H.G. & Vunjak-Novakovic, G. Electrical stimulation enhances cell migration and integrative repair in the meniscus. *Sci. Rep.* **4**, 3674; DOI:10.1038/srep03674 (2014).